# *Hydrocarbon source potential of the Tanezzuft Formation, Murzuq Basin, south-west Libya*

Diasty, W. Sh. El; El Beialy, S. Y. ; Anwari, T. A.; Batten, David

*Published in:*
Journal of African Earth Sciences

*DOI:*
10.1016/j.jafrearsci.2017.03.005

*Publication date:*
2017

*Citation for published version (APA):*
Diasty, W. S. E., El Beialy, S. Y., Anwari, T. A., & Batten, D. (2017). Hydrocarbon source potential of the Tanezzuft Formation, Murzuq Basin, south-west Libya: An organic geochemical approach. *Journal of African Earth Sciences*, *130*, 102-109. https://doi.org/10.1016/j.jafrearsci.2017.03.005

# Accepted Manuscript


Hydrocarbon source potential of the Tanezzuft Formation, Murzuq Basin, south-west Libya: An organic geochemical approach

W.Sh. El Diasty, S.Y. El Beialy, T.A. Anwari, D.J. Batten

PII: S1464343X17301097

DOI: 10.1016/j.jafrearsci.2017.03.005

Reference: AES 2841

To appear in: *Journal of African Earth Sciences*

**Highlights**

1. A wide variation of source richness and quality between Hot Shale and the Tanezzuft Formation is recognized.
2. Immature to early mature kerogen type II/III kerogen for the Hot Shale samples is reported.
3. The Tanezzuft samples are dominated by type III/II kerogen.
4. The Hot Shale and Tanezzuft Formation are of mixed organic matter input and different concentrations.

# Hydrocarbon source potential of the Tanezzuft Formation, Murzuq Basin, south-west Libya: An organic geochemical approach

W.Sh. El Diasty [1*], S.Y. El Beialy [1], T.A. Anwari [1], D.J. Batten [2]

[1] *Mansoura University, Faculty of Science, Geology Department, Mansoura 35516, Egypt*
[2] *Department of Geography and Earth Sciences, Aberystwyth University, Penglais, Aberystwyth SY23 3DB, Wales, UK, and School of Earth, Atmospheric and Environmental Sciences, University of Manchester, Oxford Road, Manchester M13 9PL, UK*

[*] Corresponding author: Dr. Waleed El Diasty, awaleed@mans.edu.eg; (+2) 0106 244 3492

**Abstract**

A detailed organic geochemical study of 20 core and cuttings samples collected from the Silurian Tanezzuft Formation, Murzuq Basin, in the south-western part of Libya has demonstrated the advantages of pyrolysis geochemical methods for evaluating the source-rock potential of this geological unit. Rock-Eval pyrolysis results indicate a wide variation in source richness and quality. The basal Hot Shale samples proved to contain abundant immature to early mature kerogen type II/III (oil–gas prone) that had been deposited in a marine environment under terrigenous influence, implying good to excellent source rocks. Strata above the Hot Shale yielded a mixture of terrigenous and marine type III/II kerogen (gas–oil prone) at the same maturity level as the Hot Shale, indicating the presence of only poor to fair source rocks.

***Keywords***: *Rock-Eval pyrolysis, Hot Shale, Tanezzuft Formation, Silurian, Murzuq Basin, Libya*

## 1. Introduction

The Murzuq Basin is one of the largest Palaeozoic intracratonic basins in the North African Sahara. It covers an area of about 350,000 square km in south-west Libya (Davidson et al., 2000), extending southwards into Niger. The focus of this study is the Silurian Tanezzuft Formation in three major oilfields, A, B and H within the NC115

Concession in the basin (Fig. 1). The lower part of the formation is referred to as the Hot Shale, a radioactive deposit that has a high gamma ray response in wireline logs, probably as a result of a high content of uranium (Fello et al., 2006). This organic-rich shale is thought to be the main source rock in the Murzuq Basin (Echikh and Sola, 2000; Sikander et al., 2000; Craig et al., 2008), and is estimated to be the origin of 80–90% of all Palaeozoic-sourced hydrocarbons in North Africa. These hydrocarbons have migrated into various reservoirs, ranging from Cambrian to Triassic sandstones that are sealed by shale intercalations. In the Murzuq Basin, Ordovician sandstones are the main reservoir rocks (Lüning et al., 2000).

The NC115 Concession is located in the north-western part of the basin, about 1,330 km south-west of Tripoli. It is about 25,850 square km in areal extent, covering approximately three-quarters of the area between 11° 30' and 12° 30'E, and 26° 8' and 26° 38'N. The B-NC115 Field is the most south-westerly of the fields examined. It is approximately 50 km to the south-west of the A-NC115 Field. This in turn is approximately 10 km west of the H-NC115 Field (Fig. 1).

The application of organic geochemical analyses of samples from the Hot Shale and overlying deposits of the Tanezzuft Formation in the NC115 Concession is reported in this paper in order to characterize the disseminated organic matter and to determine the hydrocarbon generation potential of, and depositional environments reflected by, the succession.

## 2. Geological background

The Murzuq Basin abuts the borders of Algeria, Niger and Chad. It is bounded to the north by the Al Gargaf Uplift, to the east by the Tibesti High, and to the west by the Tihemboka High (Echikh and Sola 2000). It lies to the south-east of the Ghadamis Basin, from which it is separated by the Atshan Saddle, an anticlinal structure trending approximately ENE–WSW, which leads into the western end of the Al Gargaf Uplift (Fig. 2).

The present structural framework of the basin reflects periods of uplift related to Caledonian (Late Silurian–Early Devonian), Hercynian (Late Carboniferous–Permian) and

Alpine (early Tertiary) events. The regional lineaments, NW–SE, are probably related to late Precambrian Pan-African fault systems (Fig. 3), which largely controlled the early Palaeozoic structural evolution of, and sediment accumulation in, the Murzuq Basin (Klitzsch, 1995).

Deposition of the Silurian succession began after the melting of the Late Ordovician ice sheets, which led to a major marine transgression that spread from the north, culminating in a high-stand with deposition of the Llandovery–Wenlock Tanezzuft Formation (Davidson et al., 2000). The formation was named by Desio (1936) after Wadi Tanezzuft, between Ghat and Awaynat. It includes a thick shale unit that overlies the Hirnantian (Late Ordovician) Mamuniyat Formation and underlies the Ludlow–Pridolí (Late Silurian) Akakus Formation (Fig. 4). The lower part of the Tanezzuft Formation is predominantly dark grey, fissile shale, and the upper part a monotonous argillaceous sequence interbedded with thin sandstone layers. Altogether it is more than 700 m thick in some wells in the NC115 Concession.

The basal part of the Tanezzuft Formation consists of the Hot Shale. It was referred to as Rhuddanian black shale by Hallett (2002), the Rhuddanian being the lowest stage of the Llandovery Epoch (443.8–440.8 Ma; Gradstein et al., 2012). The high level of natural radioactivity in some of the shales is the result of an increase in authigenic uranium, which is readily recognized in well logs by high gamma-ray values (up to 400 API). High gamma-ray intervals can also be related to lithologies other than hot shale, e.g., shale rich in detrital K and Th (Lüning et al., 2000; Armstrong et al., 2005). The Hot Shale consists of black, dark brown and dark grey, splintery, compact, micaceous, pyritic shale (Fig. 4). It is present only in the B42 and H39i wells, where it is up to 45 m thick. The organic matter it contains was probably a result of high algal productivity in a region of oceanic upwelling along the North Gondwanan shelf margin (Finney and Berry, 1997).

## 3. Samples and analytical procedures

Twenty core and cuttings samples of the Tanezzuft Formation, including the Hot Shale, were selected from seven wells in oilfields A, B and H in the NC-115 Concession

(Fig. 2). These were subjected to total organic carbon (TOC) and Rock-Eval pyrolysis analyses at the StratoChem Laboratory, New Maadi, Cairo (Egypt). The instrument used was a Rock-Eval 6 pyro-analyzer equipped with a TOC module. The samples were heated from 300°C (hold time 3 min) to 850°C (hold time 5 min) at 25°C/min for oxidation.

## 4. Results and discussion

The TOC/Rock-Eval analytical data on the rock samples are summarized in Table 1 and graphically represented in Figs. 5–8. The cross-plot between TOC and $S_2$ is reliable for evaluating the organic richness of a source rock (Dembicki, 2009), and the hydrogen index (HI) versus oxygen index (OI) cross-plot defines the type of kerogen present (Espitalié et al., 1977; Peters and Cassa, 1994). The cross-plot of HI versus $T_{max}$ is commonly used to avoid the influence of OI for determining thermal maturity and kerogen type (Hunt, 1996), and the relationship between the pyrolysis $T_{max}$ and production index (PI) is a valuable method for evaluating the thermal maturity of organic matter (Peters and Cassa, 1994).

As shown in Fig. 5 and Table 1, the TOC of the Hot Shale samples ranges from 1.22 to 20.90%, and $S_2$ values from 0.36 to 59.47 mg HC/g rock, whereas the overlying deposits of the Tanezzuft Formation have TOC values that range from 0.34 to 1.08%, and $S_2$ values from 0.14 to 2.78 mg HC/g rock. These data indicate the superior petroleum potential of the Hot Shale (good to excellent) by comparison with the rest of the formation (poor to fair). From a statistical point of view, shale with TOC values >3%, as for four of the six samples of the Hot Shale examined, usually contain marine organic matter, and are thus oil-prone (Demaison and Moore, 1980; Tyson, 1995; Batten, 1996).

The HI versus OI cross-plot (Fig. 6) shows that, apart from one sample, the Hot Shale deposits examined yielded Type II/III kerogen (oil/gas-prone), i.e., mixed marine and terrigenous organic matter. The exception is from well B42 at depth 4640 ft (1414 m). This contained Type III (gas-prone) kerogen, which indicates a well-oxygenated (oxic) depositional environment (Peters and Cassa, 1994). On the other hand, again with one exception, the rocks above the Hot Shale yielded Type III to II/III kerogen (gas-prone) to (oil/gas-prone). The exception is a sample from well H40 at a depth 4380 ft (1335 m) that produced an HI value of 375 mg HC/g TOC (Table 1), reflecting Type II kerogen that was probably derived from marine organic matter (Peters and Cassa, 1994).

Figs. 5 and 6 clearly separate the organic-rich Hot Shale from the organically lean deposits of the rest of the formation. The difference between the organic content and hence kerogen type in the two parts of the succession is likely to reflect variations in the supply of organic matter, and its preservation and dilution in different depositional environments.

The relationship between HI and $T_{max}$ (Fig. 7) shows that the Hot Shale and overlying deposits have $T_{max}$ values that range from 432 to 444ºC and 433 to 439ºC, respectively (Table 1), indicating an early mature stage for the samples analyzed. This is confirmed by the cross-plot of $T_{max}$ versus PI (Fig. 8), which shows that the majority of the samples lie within the zone of the early oil window.

## 5. Conclusions

The results of an analysis using TOC/Rock-Eval pyrolysis equipment of 20 cores and cuttings samples taken from the Tanezzuft Formation in the Murzuq Basin of south-west Libya are presented. The basal unit of the formation, known as the Hot Shale, reflects deposition in a marine environment under terrigenous influence. Being close to and within the early mature oil window it has generally good–excellent potential to generate both oil and gas. The rest of the formation, which overlies the Hot Shale, is of similar maturity but has more limited (poor to fair) potential to generate gas and minor oil. However, in places there are thin horizons where the shales are good oil/gas-prone source rocks. These contain kerogen types III to II/III, the organic matter having both marine and terrigenous origins. The differences in geochemical characteristics between most of the Hot Shale and the rest of the Tanezzuft Formation largely reflect differences in organic matter influx, mode of preservation and depositional environments.

## Acknowledgements

The Harouge Oil Operations is acknowledged for the provision of samples, geological information and permission to publish this paper. The authors are most grateful to StratoChem, New Maadi, Cairo, Egypt for laboratory assistance and running the organic geochemical investigation in this study. We thank the Associate Editor W. Bosworth and an anonymous reviewer for their constructive and very helpful comments on the manuscript.

**References**

Armstrong, H.A., Turner, B.R., Makhlouf, I.M., Weedon, G.P., Williams, M., Al Smadi, A., Abu Salah, A., 2005. Origin, sequence stratigraphy and depositional environment of an upper Ordovician (Hirnantian) deglacial black shale, Jordan. Palaeogeography, Palaeoclimatology, Palaeoecology 220, 273–289.

Aziz, A., 2000. Stratigraphy and hydrocarbon potential of the Lower Paleozoic succession of License NC-115, Murzuq Basin, southwest Libya. In: Sola, M.A., Worsley, D. (Eds.), Geological Exploration in the Murzuq Basin. Elsevier, Amsterdam, pp. 349–368.

Batten, D.J., 1996. Palynofacies and petroleum potential. Chapter 26B. In Jansonius, J., McGregor, D.C. (Eds.), Palynology: Principles and Applications, Volume 3. American Association of Stratigraphic Palynologists' Foundation, Dallas, pp. 1065–1084.

Craig, J., Rizzi, C., Said, F., Thusu, B., Luning, S., Asbali, A.I., Keeley, M.L., Bell, J.F., Durham, M.J., Eales, M.H., Beswetherick, S., Hamblett, C., 2008. Structural styles and prospectivity in the Precambrian and Paleozoic hydrocarbon systems of North Africa. In: Salem, M.J., Oun, K.M., Essed, A.S. (Eds.), The Geology of East Libya, Vol. 4. Gutenberg Press, Malta, pp. 51–122.

Davidson, L., Beswetherick, S., Craig, J., Eales, M., Fisher, A., Himmali, A., Jho, J., Mejrab, B., Smart, J., 2000. The structure, stratigraphy and petroleum geology of the Murzuq Basin, southwest Libya. In: Sola, M.A., Worsley, D. (Eds.), Geological Exploration in the Murzuq Basin. Elsevier, Amsterdam, pp. 295–320.

Demaison, G.J., Moore, G. T., 1980. Anoxic environments and oil source bed genesis. American Association of Petroleum Geologists, Bulletin 64, 1179–1209.

Dembicki, H.J., 2009. Three common source rock evaluation errors made by geologists during prospect or play appraisals. American Association of Petroleum Geologists, Bulletin 93, 341–356.

Desio, A., 1936. Riassunto sulla presenza del Silurico fossilifero nel Fezzan. Bollettino. Societa Geologica Italiana 55, 319–356.

Echikh, K., Sola, M.A., 2000. Geology and hydrocarbon occurrences in the Murzuq Basin, SW Libya. In: Sola, M.A., Worsley, D. (Eds.), Geological Exploration in the Murzuq Basin. Elsevier, Amsterdam, pp. 175–222.

Espitalié, J., Laporte, J.L., Madec, M., Marquis, F., Leplat, P., Paulet, J., Boutefeu, A., 1977. Méthode rapide de caractérisation des roches mères, de leur potential pétrolier et de leur degré d'évolution. Revue de l'Institut Français du Pétrole 32, 23–42.

Fello, N., Lüning, S., Storch, P., Redfern, J., 2006. Identification of early Llandovery (Silurian) anoxic palaeo-depressions at the western margin of the Murzuq Basin, (S.W. Libya) based on gamma-ray spectrometry in surface exposures. GeoArabia 11, 101–118.

Finney, S.C., Berry, W.B.N., 1997. New perspectives on graptolite distributions and their use as indicators of platform margin dynamics. Geology 25, 919–922.

Gradstein, F.M., Ogg, J.G., Hilgen, F.J., 2012. On the geologic time scale. Newsletters on Stratigraphy 45, 171–188.

Hallet, D., 2002. Petroleum Geology of Libya. Elsevier, Amsterdam, 503 p.

Hunt, J.M., 1996. Petroleum Geochemistry and Geology. 2nd edition. W.H. Freeman, New York, 743 p.

Klitzsch, E., 1995. Libyan/Libya. In: Kulke, H. (Ed.), Regional Petroleum Geology of the World, Part II. Contributions to Regional Geology and Development, 22. Borntrager, Stuttgart, pp. 45–56.

Lüning, S., Craig, J., Loydell, D.K., Storch, P., Fitches, W.R., 2000. Lower Silurian 'hot shales' in North Africa and Arabia: regional distribution and depositional model. Earth Science Reviews 49, 121–200.

Peters, K.E., Cassa, M.R., 1994. Applied source-rock geochemistry. In: Magoon, L.B., Dow, W.G. (Eds.), The Petroleum System – From Source to Trap. American Association of Petroleum Geologists, Memoir 60, 93–120.

Sikander, A.H., Basu, S., Rasul, S.M., 2000. Geochemical source-maturation and volumetric evaluation of Lower Paleozoic source rocks in the west Libyan basins. In: Salem, M.J., Oun, K.M., Seddiq, H.M. (Eds.), The Geology of Northwest Libya 3, pp. 3–53.

Tyson, R.V., 1995. Sedimentary Organic Matter: Organic Facies and Palynofacies. Chapman and Hall, London. 614 p.

**Figure and Table captions**

**Fig. 1.** Location of the A, B and H fields in the NC115 Concession of the Murzuq Basin and of the samples within these fields.

**Fig. 2.** Map of the tectonic elements in the Murzuq Basin (after Echikh and Sola, 2000).

**Fig. 3.** Schematic cross-section through the Murzuq Basin showing major structures, three tectonic unconformities and eroded sedimentary sequences: Unc, unconformity (after Davidson et al., 2000).

**Fig. 4.** Subsurface stratigraphic chart for the Murzuq Basin (substantially modified after Aziz, 2000; Gradstein et al., 2012).

**Fig. 5.** Organic richness based on TOC content and $S_2$ values of samples from the Tanezzuft Formation including the Hot Shale, plotted separately.

**Fig. 6.** HI versus OI of samples from the Tanezzuft Formation including the Hot Shale, plotted separately.

**Fig. 7.** HI versus $T_{max}$ of samples from the Tanezzuft Formation including the Hot Shale, plotted separately.

**Fig. 8.** $T_{max}$ versus PI of samples from the Tanezzuft Formation including the Hot Shale, plotted separately.

**Table 1.** TOC % and Rock-Eval pyrolysis results of samples from the Tanezzuft Formation.

**Figure 1**

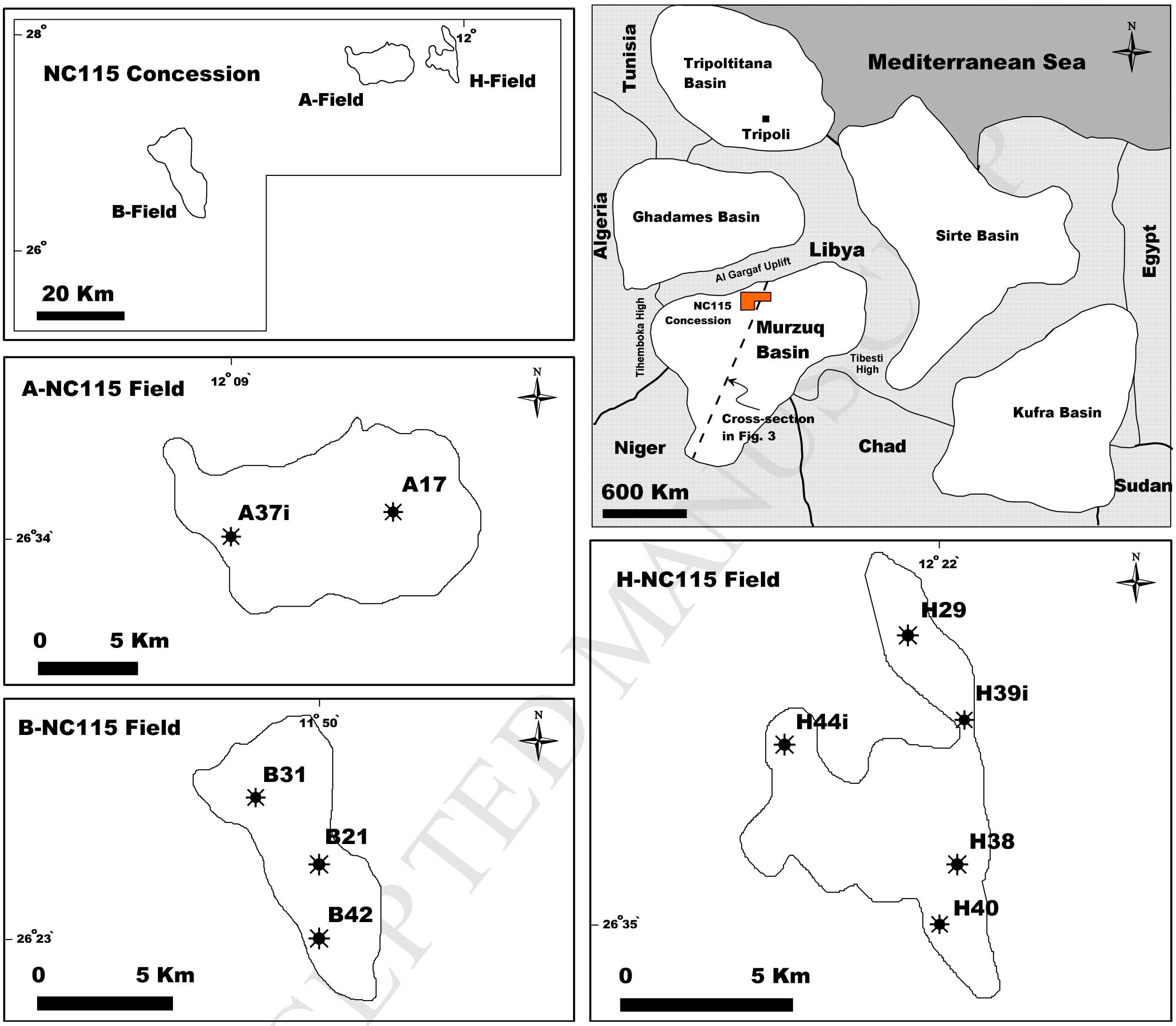
NC115 Concession
A-Field
H-Field
B-Field
28°
26°
12°
20 Km
A-NC115 Field
12° 09`
26°34`
A37i
A17
0 5 Km
B-NC115 Field
11° 50`
26°23`
B31
B21
B42
0 5 Km
Tunisia
Tripoltitana Basin
Tripoli
Mediterranean Sea
Algeria
Ghadames Basin
Al Gargaf Uplift
Libya
Sirte Basin
Egypt
NC115 Concession
Murzuq Basin
Tihemboka High
Tibesti High
Cross-section in Fig. 3
Niger
Chad
Kufra Basin
Sudan
600 Km
H-NC115 Field
12° 22`
H29
H39i
H44i
H38
H40
26°35`
0 5 Km

**Figure 2**

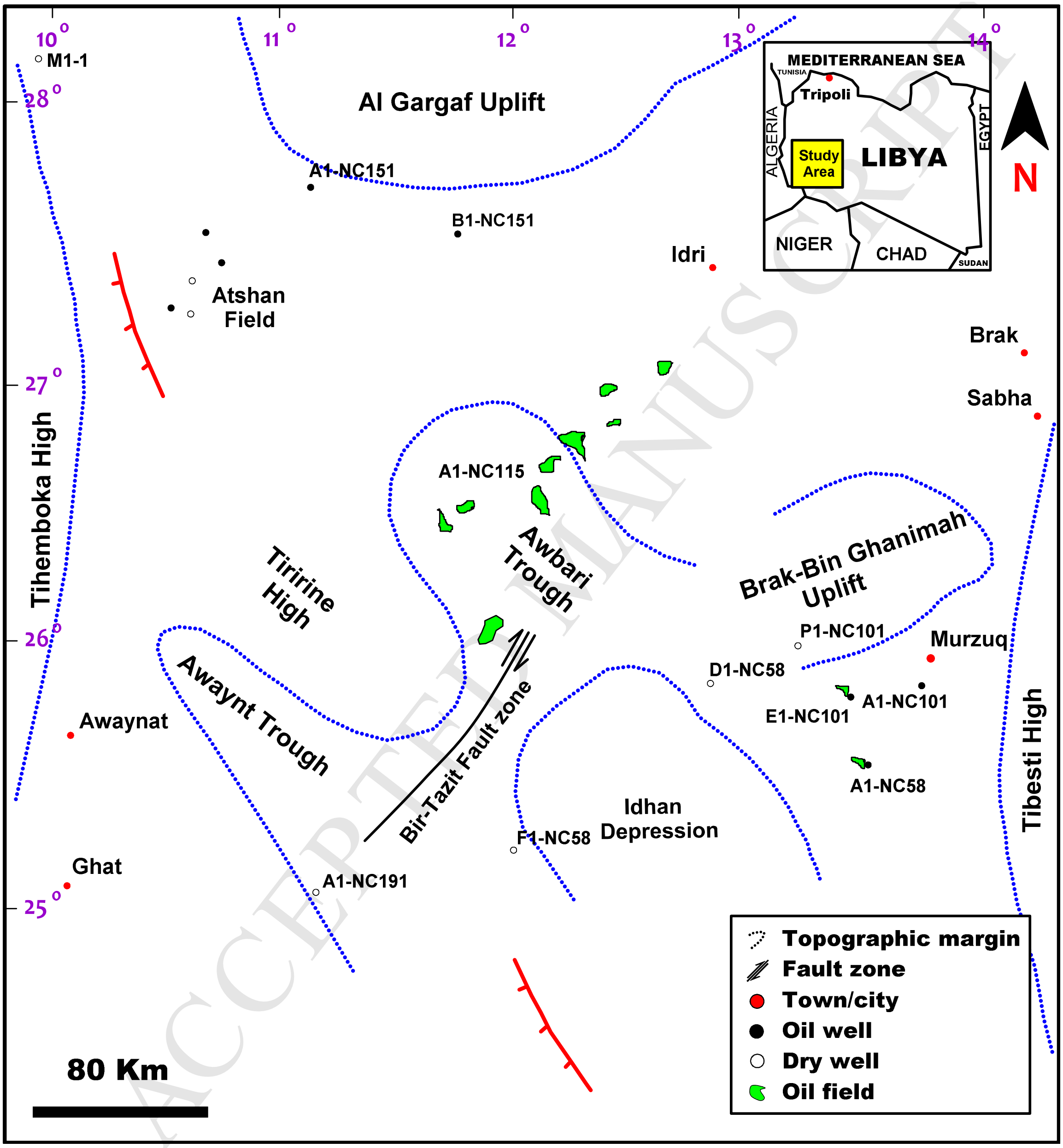
10°
11°
12°
13°
14°
28°
27°
26°
25°
M1-1
Al Gargaf Uplift
A1-NC151
B1-NC151
Idri
Atshan
Field
Brak
Sabha
A1-NC115
Tihemboka High
Tiririne
High
Awbari
Trough
Brak-Bin Ghanimah
Uplift
P1-NC101
Murzuq
D1-NC58
A1-NC101
E1-NC101
Awaynat
Awaynt Trough
Bir-Tazit Fault zone
A1-NC58
Tibesti High
Idhan
Depression
F1-NC58
Ghat
A1-NC191
MEDITERRANEAN SEA
TUNISIA
Tripoli
ALGERIA
EGYPT
Study
Area
LIBYA
NIGER
CHAD
SUDAN
N
Topographic margin
Fault zone
Town/city
Oil well
Dry well
Oil field
80 Km

**Figure 3**

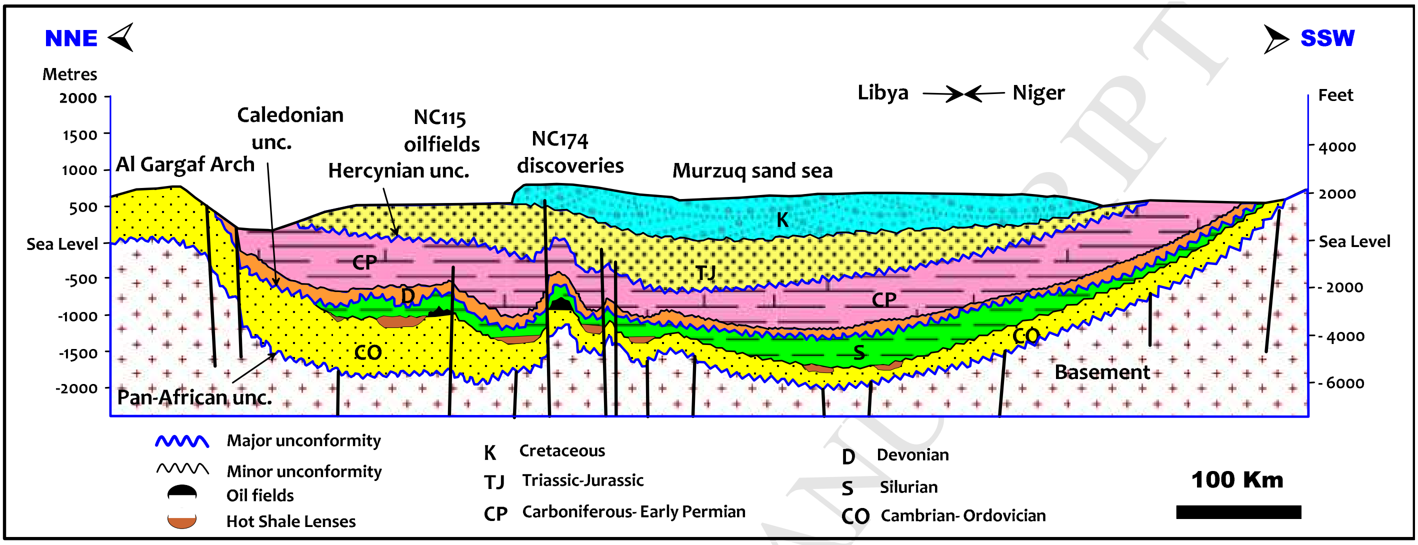
NNE
SSW
Metres
2000
1500
1000
500
Sea Level
-500
-1000
-1500
-2000
Feet
4000
2000
Sea Level
- 2000
- 4000
- 6000
Libya
Niger
Caledonian unc.
NC115 oilfields
NC174 discoveries
Al Gargaf Arch
Hercynian unc.
Murzuq sand sea
K
CP
TJ
D
CO
S
Basement
Pan-African unc.
Major unconformity
Minor unconformity
Oil fields
Hot Shale Lenses
K Cretaceous
TJ Triassic-Jurassic
CP Carboniferous- Early Permian
D Devonian
S Silurian
CO Cambrian- Ordovician
100 Km

**Figure 4**

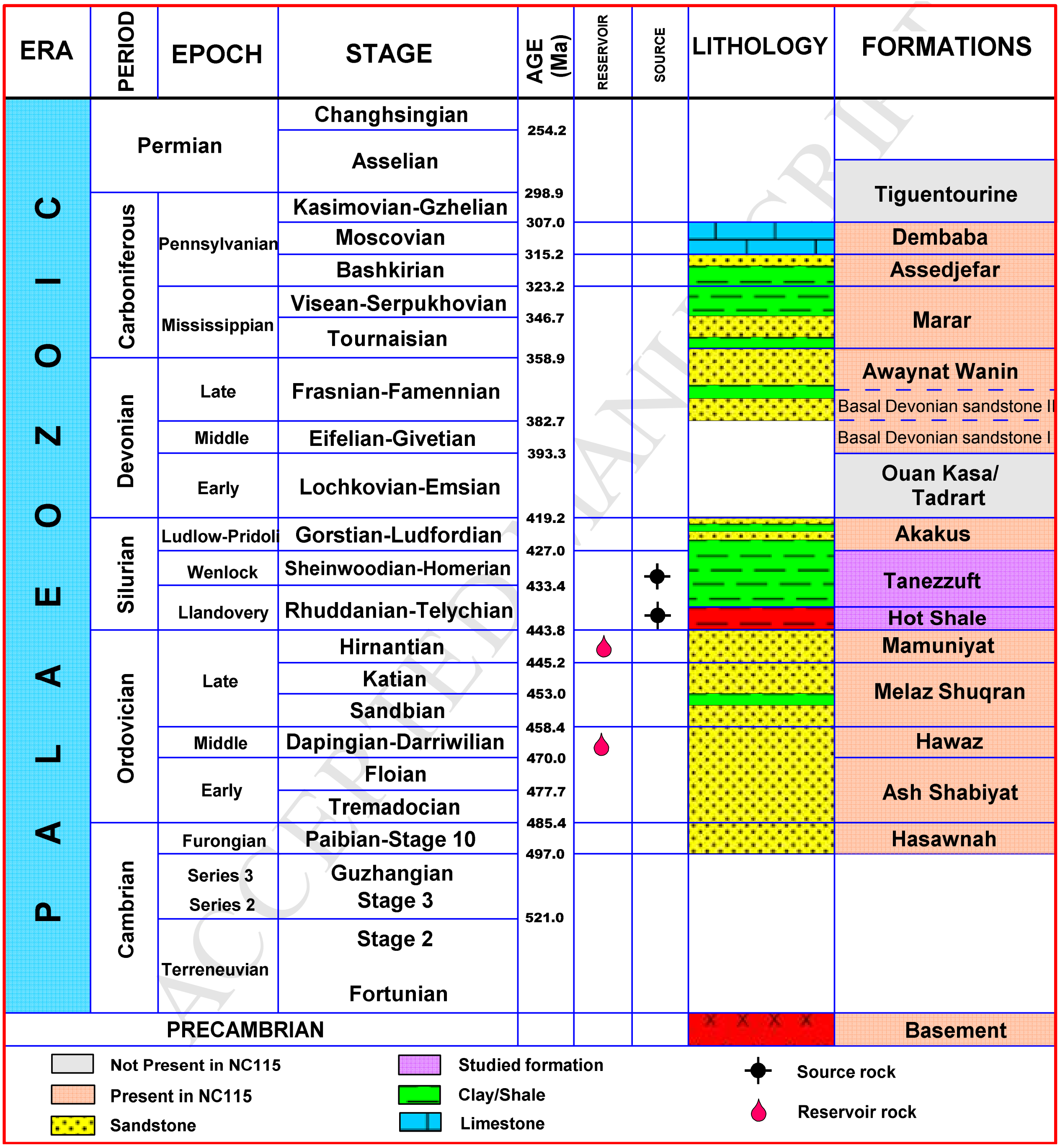
ERA
PERIOD
EPOCH
STAGE
AGE (Ma)
RESERVOIR
SOURCE
LITHOLOGY
FORMATIONS
P A L A E O Z O I C
Permian
Changhsingian
Asselian
254.2
298.9
Carboniferous
Pennsylvanian
Kasimovian-Gzhelian
Moscovian
Bashkirian
Mississippian
Visean-Serpukhovian
Tournaisian
307.0
315.2
323.2
346.7
358.9
Devonian
Late
Frasnian-Famennian
Middle
Eifelian-Givetian
Early
Lochkovian-Emsian
382.7
393.3
419.2
Silurian
Ludlow-Pridoli
Gorstian-Ludfordian
Wenlock
Sheinwoodian-Homerian
Llandovery
Rhuddanian-Telychian
427.0
433.4
443.8
Ordovician
Late
Hirnantian
Katian
Sandbian
Middle
Dapingian-Darriwilian
Early
Floian
Tremadocian
445.2
453.0
458.4
470.0
477.7
485.4
Cambrian
Furongian
Paibian-Stage 10
Series 3
Series 2
Guzhangian
Stage 3
Terreneuvian
Stage 2
Fortunian
497.0
521.0
PRECAMBRIAN
Tiguentourine
Dembaba
Assedjefar
Marar
Awaynat Wanin
Basal Devonian sandstone II
Basal Devonian sandstone I
Ouan Kasa/ Tadrart
Akakus
Tanezzuft
Hot Shale
Mamuniyat
Melaz Shuqran
Hawaz
Ash Shabiyat
Hasawnah
Basement
Not Present in NC115
Present in NC115
Sandstone
Studied formation
Clay/Shale
Limestone
Source rock
Reservoir rock

**Figure 5**

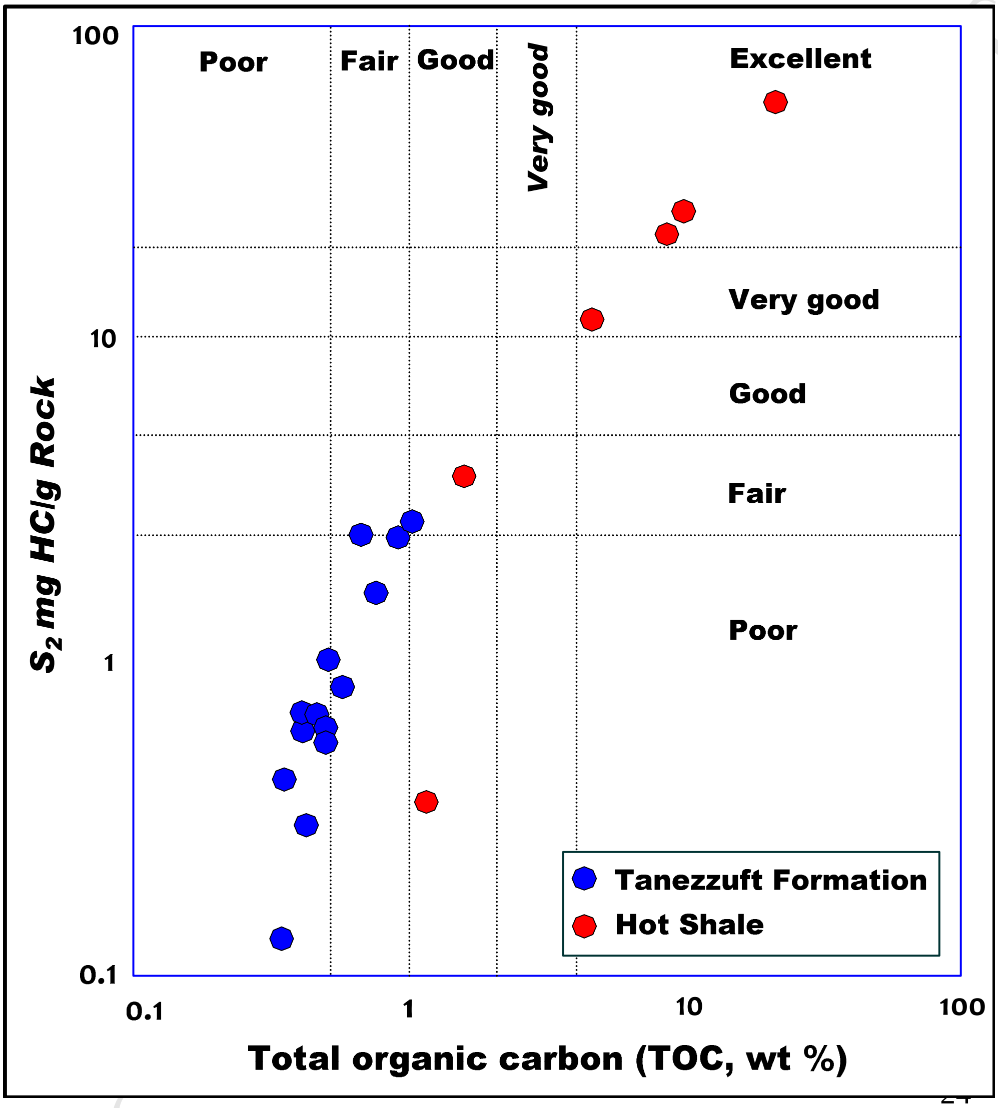

100
10
1
0.1
0.1
1
10
100
$S_2$ mg HC/g Rock
Total organic carbon (TOC, wt %)
Poor
Fair
Good
Very good
Excellent
Very good
Good
Fair
Poor
Tanezzuft Formation
Hot Shale

**Figure 6**

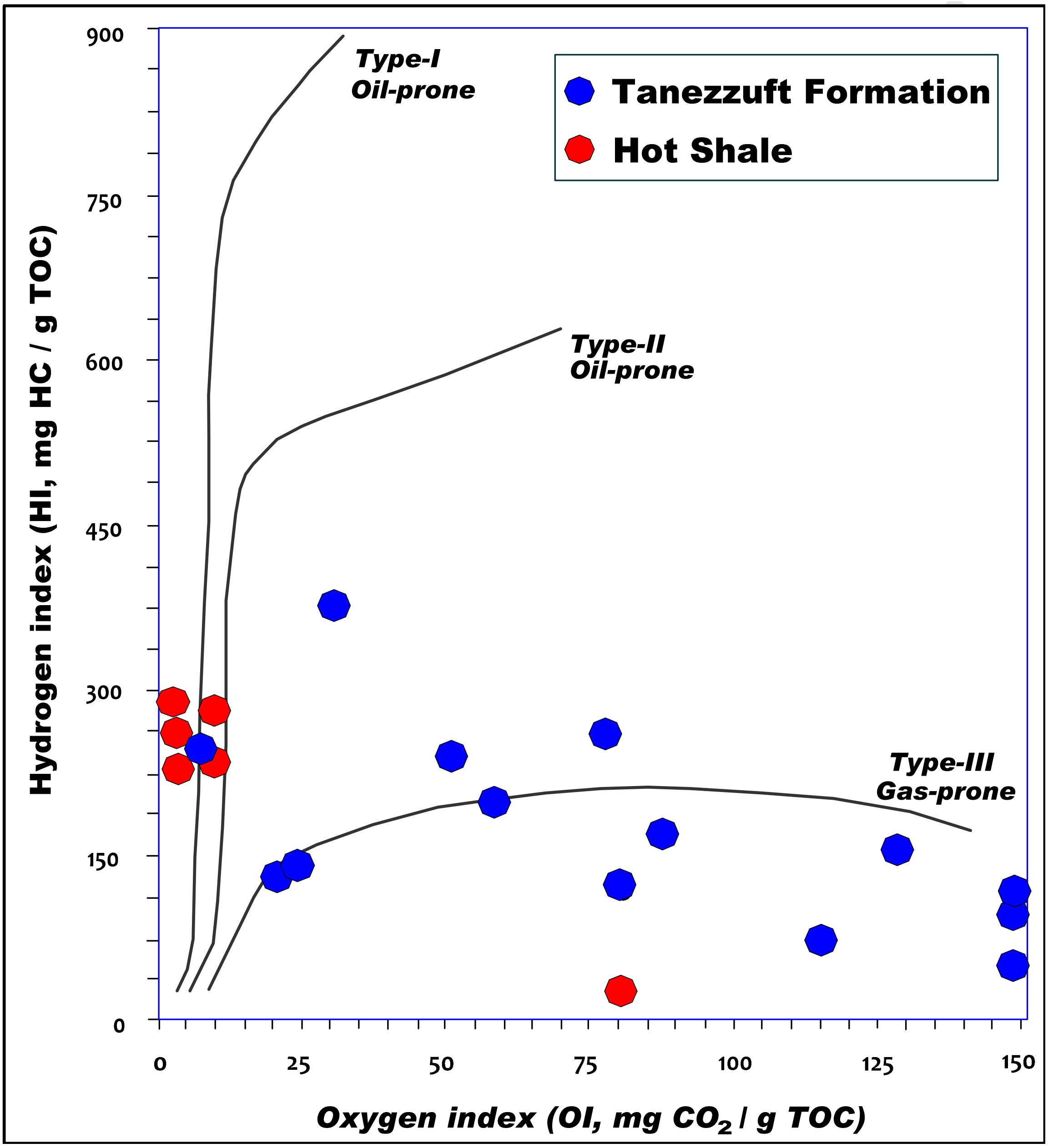
Tanezzuft Formation
Hot Shale
Type-I
Oil-prone
Type-II
Oil-prone
Type-III
Gas-prone
Hydrogen index (HI, mg HC / g TOC)
900
750
600
450
300
150
0
0
25
50
75
100
125
150
Oxygen index (OI, mg CO2 / g TOC)

**Figure 7**

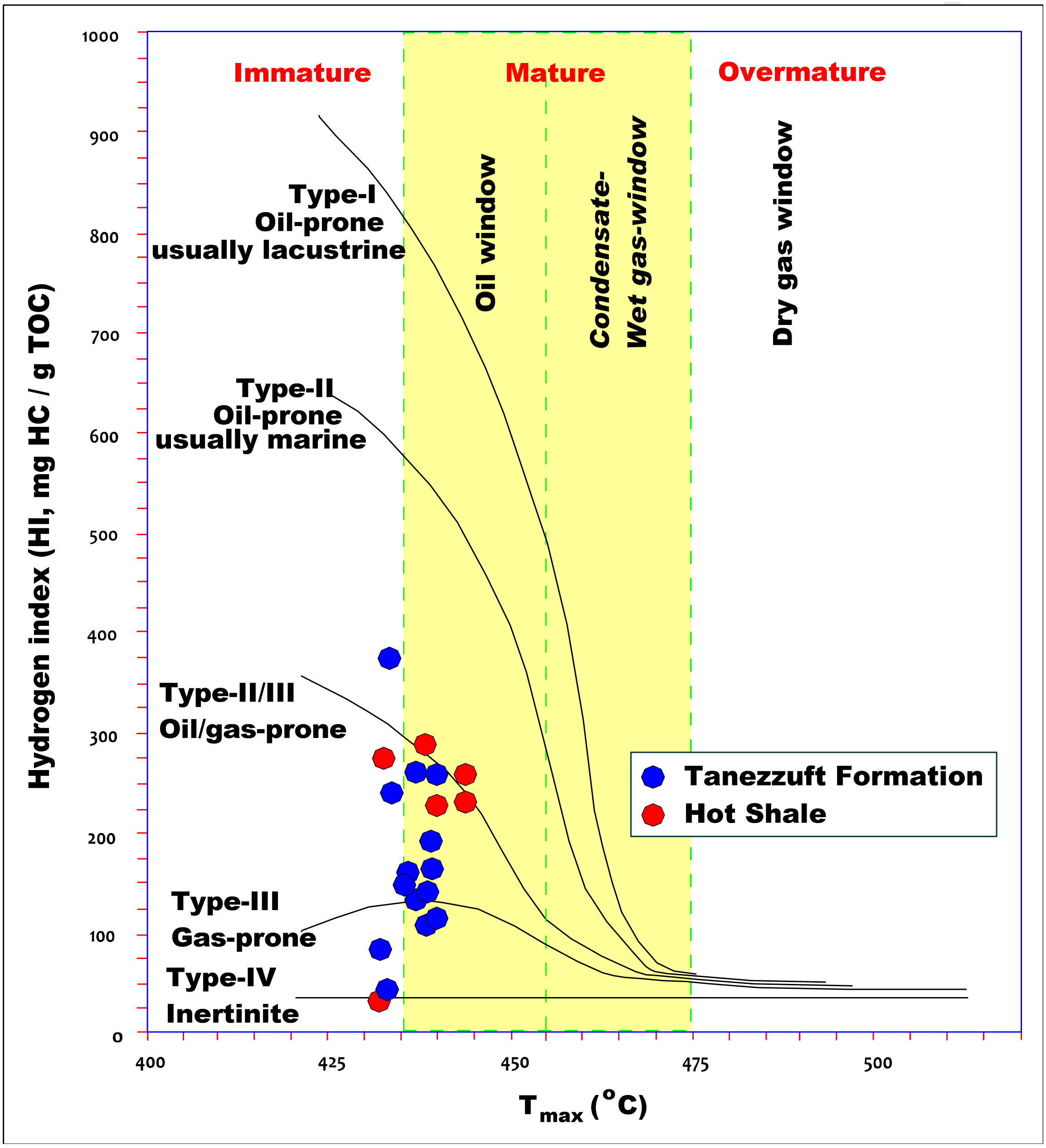
Immature
Mature
Overmature
Type-I
Oil-prone
usually lacustrine
Type-II
Oil-prone
usually marine
Type-II/III
Oil/gas-prone
Type-III
Gas-prone
Type-IV
Inertinite
Oil window
Condensate-
Wet gas-window
Dry gas window
Tanezzuft Formation
Hot Shale
Hydrogen index (HI, mg HC / g TOC)
0
100
200
300
400
500
600
700
800
900
1000
400
425
450
475
500
T max (°C)

**Figure 8**

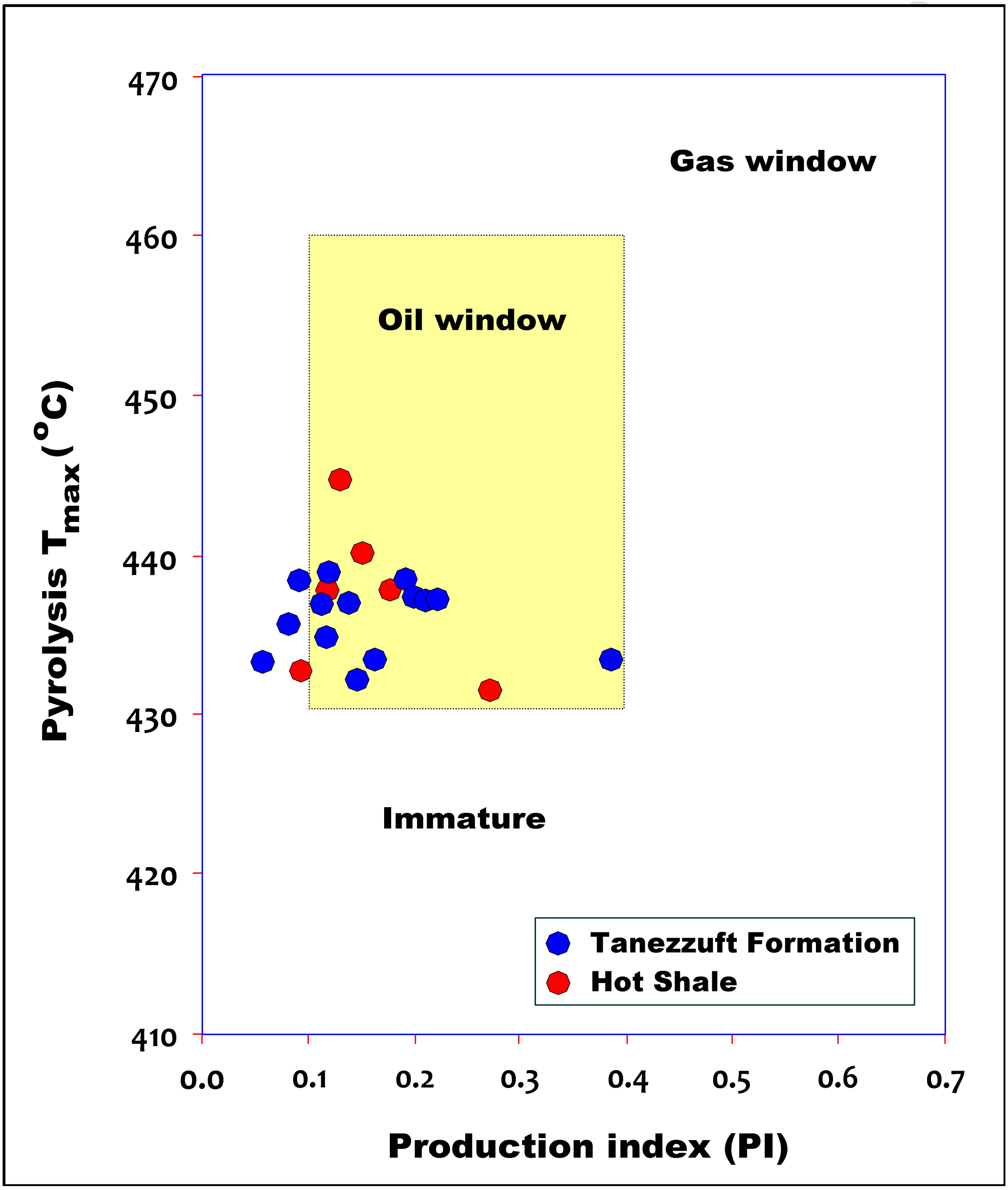

Pyrolysis $T_{max}$ (°C)
470
460
450
440
430
420
410
Gas window
Oil window
Immature
Tanezzuft Formation
Hot Shale
0.0
0.1
0.2
0.3
0.4
0.5
0.6
0.7
Production index (PI)

**Table 1**

| **Well name** | **Rock-unit** | **Sample type** | **Depth (m)** | **TOC wt%** | **$S_1$ mg/g** | **$S_2$ mg/g** | **$S_3$ mg/g** | **$T_{max}$ (°C)** | **HI mg HC/g TOC** | **OI mg HC/g TOC** | **PI** |
|---|---|---|---|---|---|---|---|---|---|---|---|
| B31 | Tanezzuft Formation | Cores | 1409 | 0.90 | 0.58 | 2.35 | 0.19 | 437 | 262 | 21 | 0.20 |
| | | | 1410 | 1.08 | 0.67 | 2.78 | 0.09 | 439 | 257 | 8 | 0.19 |
| A17 | | | 1479 | 0.48 | 0.15 | 0.61 | 0.10 | 437 | 128 | 21 | 0.20 |
| | | | 1481 | 0.57 | 0.21 | 0.79 | 0.13 | 438 | 138 | 23 | 0.21 |
| H39i | | Cuttings | 1213 | 0.40 | 0.05 | 0.60 | 0.51 | 436 | 152 | 129 | 0.08 |
| A37 | | | 1298 | 0.40 | 0.05 | 0.31 | 0.46 | 433 | 77 | 115 | 0.14 |
| | | | 1380 | 0.40 | 0.07 | 0.67 | 0.35 | 439 | 169 | 88 | 0.09 |
| | | | 1463 | 0.48 | 0.08 | 0.55 | 0.39 | 438 | 114 | 81 | 0.13 |
| B42 | | | 1185 | 0.73 | 0.10 | 1.75 | 0.38 | 434 | 239 | 52 | 0.05 |
| | | | 1286 | 0.42 | 0.08 | 0.67 | 0.32 | 436 | 161 | 77 | 0.11 |
| | | | 1395 | 0.34 | 0.09 | 0.14 | 0.50 | 433 | 42 | 149 | 0.39 |
| H40 | | | 1225 | 0.35 | 0.05 | 0.40 | 0.67 | 438 | 114 | 191 | 0.11 |
| | | | 1335 | 0.68 | 0.53 | 2.56 | 0.21 | 434 | 375 | 31 | 0.17 |
| | | | 1438 | 0.51 | 0.14 | 0.99 | 0.30 | 439 | 195 | 59 | 0.12 |
| B42 | Hot Shale | | 1414 | 1.22 | 0.13 | 0.36 | 0.99 | 432 | 30 | 81 | 0.27 |
| H39i | | | 1449 | 9.70 | 2.58 | 26.63 | 0.98 | 433 | 275 | 10 | 0.09 |
| H29 | | Cores | 1473 | 4.86 | 1.96 | 11.04 | 0.21 | 440 | 227 | 4 | 0.15 |
| | | | 1477 | 8.61 | 2.98 | 22.58 | 0.23 | 444 | 262 | 3 | 0.12 |
| | | | 1482 | 20.9 | 7.42 | 59.47 | 0.33 | 438 | 285 | 2 | 0.11 |
| | | | 1487 | 1.71 | 0.84 | 3.90 | 0.17 | 438 | 228 | 10 | 0.18 |

**TOC** = Total organic carbon as weight percent organic carbon in rock; **$S_1$** = Free hydrocarbons emitted from rock without cracking of kerogen (mg hydrocarbons per gram of rock); **$S_2$** = Residual hydrocarbons representing the remaining generative hydrocarbon potential (mg hydrocarbons per gram of rock); **$S_3$** = Generated carbon dioxide (mg carbon dioxide per gram of rock); **$T_{max}$** = Temperature reached during maximum generation of hydrocarbons measured via $S_2$ peak of Rock-Eval pyrolysis ($^o$C); **HI** = Hydrogen index = $S_2$×100/TOC; **OI** = Oxygen index = $S_3$×100/TOC; **PI** = Production index = $S_1/(S_1+S_2)$.